05,10

Nonlinear inertial dynamics of the magnetization of antiferromagnets and dynamic magnetic hysteresis

© A.S. Titov[1], N.V. Chukashev[1], S.V. Titov[2]

[1] Center for Photonics and 2D Materials, Moscow Institute of Physics and Technology, Dolgoprudnyi, Russia
[2] Fryazino Branch, Kotel'nikov Institute of Radio Engineering and Electronics, Russian Academy of Sciences, Fryazino, Moscow oblast, Russia

E-mail: titov.as@phystech.edu

Received July 23, 2025
Revised August 20, 2025
Accepted August 30, 2025

The nonlinear response of magnetization of antiferromagnetic nanoparticles under the action of an alternating magnetic field of extremely high frequency is investigated. The case of uniaxial magnetic anisotropy of antiferromagnet sublattices with a uniform external field imposed along the easy axis is considered. The solution of the inertial Landau–Lifshitz–Gilbert equation by the method of successive approximations made it possible to obtain analytical expressions for the components of the nonlinear magnetic susceptibility tensor of the second and third orders. The dynamic magnetic hysteresis at extremely high frequencies in the nutation resonance region is calculated. It is shown that both the nonlinear susceptibility and the shape of the hysteresis loop in the THz frequency range significantly depend on the frequency of the alternating field, as well as on the inertial relaxation time. It has been demonstrated that such nonlinear effects as frequency doubling and the appearance of weak subharmonic resonance peaks observed in the frequency region of antiferromagnetic resonance are also reproduced in the region of nutation resonance.

Keywords: antiferromagnet, ferromagnet, nutation resonance, antiferromagnetic resonance, Landau–Lifshitz–Gilbert equation, magnetization inertia, uniaxial magnetocrystalline anisotropy.

DOI: 10.61011/PSS.2025.09.62355.211-25

1. Introduction

Antiferromagnets (AFMs) are increasingly utilized in modern technologies and are an object of research in the important field of antiferromagnetic spintronics [1–6].The AFMs are magnetic materials, in which an average magnetic moment is either zero or quite small as compared to magnetic moments that are inside these materials [7]. It is important to study magnetization dynamics of AFMs for developing spintronics, magnonics and other fields of science, technology and biomedicine [8–10].The AFMs can be insulators, metals, semimetals or semiconductors and are much more widespread than ferromagnetics (FM), which are mainly metals [11]. The AFMs can be both natural and artificially made. Low magnetization in the natural AFMs can be a result of slight asymmetry in a geometry of almost collinear magnetizations of AFM spin sublattices. The so-called „synthetic" AFMs are usually artificial materials with layers of the ferromagnetic type coupled by interaction. Antiparallel magnetizations of the spin sublattices in the AFMs mean insensitivity to parasitic magnetic fields [12], which is one of the advantages of these materials. Another useful property of the AFMs is faster spin dynamics than in the FMs [13]. Thus, due to strong exchange interaction between the spin sublattices antiferromagnetic resonance can be observed within the terahertz frequency range [14,15], whereas due to a weaker field induced by magnetic anisotropy ferromagnetic resonance is within the gigahertz frequency range [13,15]. Currently, magnetic nanostructures that enable superfast remagnetization are in high demand in new technological developments. At the same time, the inertia of magnetization plays a significant role in superfast dynamic processes [16,17].

It was shown by theoretical studies [18–22] that inertia of magnetization resulted in nutation motion of a magnetization vector, which is superimposed on its regular precession around an effective field. Nutation of magnetization is manifested as nutation resonance (NR) in the FMs [22–25] and the AFMs [25–27] in the terahertz (THz) frequency range as well as nutation waves [28–30]. Inertial dynamics of magnetization is experimentally confirmed in the studies [31,32], which describe NR induced by inertia of magnetization and observed in thin ferromagnetic films of NiFe, CoFeB and Co at THz frequencies. Theoretical studies of inertial dynamics of magnetization are based on the Landau–Lifshitz–Gilbert (LLG) equation that is supplemented with an inertial term. At the microscopic level various theoretical models have been developed, which utilize the inertial LLG equation. In particular, they include studies based on calculation of a torque correlation [33], on generalization of the Fermi surface model [34], on application of the electronic structure analysis method [35], on consideration of relativistic spin dynamics [36,37], and others. For example, it is shown in Ref. [36] that the inertial

term appears in the generalized LLG equation as a result of taking into account higher-order relativistic terms when considering spin-orbit interaction as compared to those that result in Gilbert decay.

In the case of AFMs, the dynamics of the magnetization of its sublattices is described by using a system of coupled inertial LLG equations. Below, for simplicity, we consider the AFMs with two identical sublattices, for which the inertial LLG equations are written [25,27] as

$$\dot{\mathbf{M}}_i = \gamma[\mathbf{H}_i^{eff} \times \mathbf{M}_i] + \frac{\alpha}{M_0}[\mathbf{M}_i \times \dot{\mathbf{M}}_i] + \frac{\tau}{M_0}[\mathbf{M}_i \times \ddot{\mathbf{M}}_i], \tag{1}$$

where $\mathbf{M}_i$ is the magnetization of the i-th sublattice (i), $i = 1, 2$, γ is the gyromagnetic ratio, α is the damping parameter, τ is the inertial relaxation time, $M_0 = |\mathbf{M}_i|$ is the absolute value of magnetization vectors of the identical sublattices of the ideal AFM, which does not change during motion. The effective field of each of the sublattices $\mathbf{H}_i^{eff}$ is the sum of several fields. Along with the external magnetic dc $\mathbf{H}_0$ and ac $\mathbf{H}_{ac}$ fields and the magnetic anisotropy field $\mathbf{H}_K$, it also includes the field $\mathbf{H}_\Lambda$ due to the exchange interaction of sublattices, namely

$$\mathbf{H}_i^{eff} = \mathbf{H}_0 + \mathbf{H}_{ac} + \mathbf{H}_K^i + \mathbf{H}_\Lambda^i.$$

If the value of the external ac field is small $h = H_{ac}/H_K \ll 1$, where $H_{ac} = |\mathbf{H}_{ac}|$ and H_K is a maximum value of the anisotropy field $\mathbf{H}_K$, then Eq. (1) can be solved using linear response theory that is based on a linear dependence between the value of the ac field and the total AFM magnetization $\mathbf{M}(t)$ and thus obtain expressions for the tensor of linear magnetic susceptibility of the AFM [27]. In strong ac fields, the linear dependence between the field and the magnetization is not fulfilled due to nonlinearity of the inertial LLG equation. In this case, a stationary response of the magnetization to the ac field results in oscillations not only at the field frequency as in the linear case, but also at harmonics of the fundamental frequency, as well as other nonlinear effects [7,38]. With significant amplitudes of the external field, it is necessary to take into account the nonlinear effects for more accurate calculations of the components of the AFM susceptibility tensor, the loop and area of dynamic magnetic hysteresis (DMH), birefringence induced by a filed and in some other applications [38–46], in which along with the amplitude, the frequency of the external ac field plays an important role. Of particular interest is the case of superposition of a dc field on the strong ac field and its ability to vary the response characteristics and manifest other effects [47].

The appearance of NR in the THz spectrum range results in DMH at these frequencies. Although the nonlinear effects and DMH in the non-inertial case have been quiet well studied, particularly in thermal noise conditions [44–54], such studies were performed in the inertial case at frequencies in the NR range only for ferromagnetic particles [38]. This study is also dedicated to investigating the nonlinear susceptibility of AFM DMH at the extremely high frequencies in the NR range. Nonlinear corrections to a linear part of the AFM susceptibility are calculated by solving the inertial LLG equation by a method of successive approximations with preservation of second- and third-order terms. It also includes analysis of the influence of inertia, the dc field value and the ac field frequency on magnetic susceptibility and DMH within the THz frequency range.

2. Dynamics of AFM magnetization in the strong ac field

The effective magnetic field of the i-sublattice in the Eq. (1) is determined as

$$\mathbf{H}_i^{eff}(t) = -\frac{1}{\mu_0}\frac{\partial V(\mathbf{M}_1, \mathbf{M}_2, t)}{\partial \mathbf{M}_i}, \tag{2}$$

where μ_0 is the permeability of free space in SI units, and $V(\mathbf{M}_1, \mathbf{M}_2, t)$ is the AFM magnetic energy per unit volume [7]. For simplicity, we consider below the AFMs with sublattices that have uniaxial magnetic anisotropy. In this case, the function $V(\mathbf{M}_1, \mathbf{M}_2, t)$ is written as

$$V(\mathbf{M}_1, \mathbf{M}_2, t) = \frac{\Lambda}{M_0^2}\mathbf{M}_1\mathbf{M}_2 - \sum_{i=1,2}\left(K\frac{(\mathbf{M}_i\mathbf{e}_Y)^2}{M_0^2} + \mu_0 H_0(\mathbf{e}_Y\mathbf{M}_i) + \mu_0 H_{ac}e^{i\omega t}(\mathbf{e}_Z\mathbf{M}_i)\right), \tag{3}$$

where H_0 is the value of the dc magnetic field, H_{ac} is the amplitude of the ac field, ω is the frequency of the ac field, Λ is the intersublattice exchange coupling parameter, K is a constant of uniaxial magnetic anisotropy of the sublattices, and, $\mathbf{e}_X, \mathbf{e}_Y$ and $\mathbf{e}_Z$ are unit vectors along the X, Y and Z axes. The geometry of the problem is shown in Figure 1, where axes of symmetry (easy axes) of the sublattices and the dc field $\mathbf{H}_0 = H_0\mathbf{e}_Y$ are oriented along the Y axis, while the ac field is directed across the easy axis $\mathbf{H}_{ac}(t) = H_{ac}e^{i\omega t}\mathbf{e}_Z$. The three-dimensional surface shown in Figure 1 is determined as the surface of a constant value of the function

$$F(\vartheta, \varphi) = \bar{V}(\vartheta, \pi - \vartheta, \varphi, \pi + \varphi) - \bar{V}(\vartheta_1^0, \vartheta_2^0, \varphi_1^0, \varphi_2^0),$$

where the function $\bar{V}$ is determined by the Eq. (3) without taking into account the variable field. Below, we consider the case of a relatively small dc field, namely $0 < H_0 < \sqrt{2(K + \Lambda)/(\mu_0 M_0)}$, at which positions of maximums of the functions $\bar{V}$ are defined by the angles $\vartheta_1^0 = \vartheta_2^0 = \pi/2$, $\varphi_1^0 = \pi/2$ and $\varphi_2^0 = 3\pi/2$ [27].

Since orientation of each of the vectors $\mathbf{M}_i$ is unambiguously determined by a pair of spherical coordinates (ϑ_i, φ_i), then, taking into account Eq. (2), Eq. (1) can be represented in spherical coordinates as a system of four

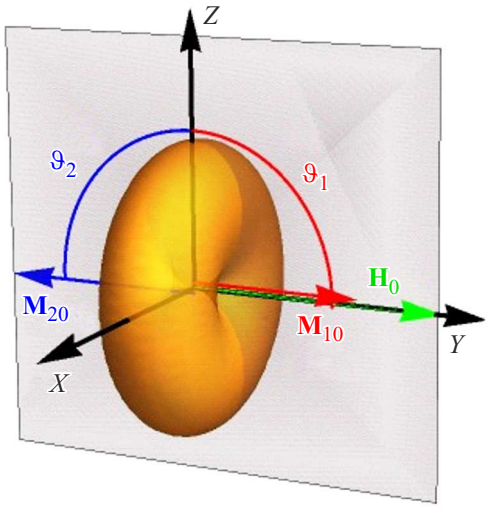

Figure 1. Geometry of the problem: the easy axis of the internal potential is directed along the Y axis, while the external dc and ac fields are defined as and $\mathbf{H}_{ac}(t) = H_{ac}e^{i\omega t}\mathbf{e}_Z$ fields are defined as.

scalar equations [5]

$$\tau\ddot{\vartheta}_i + \alpha\dot{\vartheta}_i - \dot{\varphi}_i \sin\vartheta_i - \tau\dot{\varphi}_i^2 \cos\vartheta_i \sin\vartheta_i + \partial_{\vartheta_i} U = 0, \quad (4)$$

$$\tau\ddot{\varphi}_i \sin\vartheta_i + \alpha\dot{\varphi}_i \sin\vartheta_i + \dot{\vartheta}_i + 2\tau\dot{\vartheta}_i\dot{\varphi}_i \cos\vartheta_i + \csc\vartheta_i \partial_{\varphi_i} U = 0, \quad (5)$$

where $U \equiv \gamma V/\mu_0 M_0$ is a normalized density of magnetic energy (3) and $i = 1, 2$. The function U is conveniently written as a sum of two terms $U = \bar{U} + \tilde{U}e^{i\omega t}$, where

$$\tilde{U} = -\omega_{ac} \sum_{i=1,2} \cos\vartheta_i \quad (6)$$

is a density of Zeeman energy due to interaction of magnetizations of the sublattices with the external ac field, while the function $\bar{U}$ includes all other types of potential energies and is defined as

$$\bar{U} = \omega_\Lambda \big(\sin\vartheta_1 \sin\vartheta_2 \cos(\varphi_1 - \varphi_2) + \cos\vartheta_1 \cos\vartheta_2\big) - \sum_{i=1,2} \left(\frac{\omega_K}{2} \sin^2\vartheta_i \sin^2\varphi_i + \omega_0 \sin\vartheta_i \sin\varphi_i\right). \quad (7)$$

Parameters $\omega_\Lambda = \gamma H_\Lambda = \gamma\Lambda/(\mu_0 M_0)$, $\omega_K = \gamma H_K = 2\gamma K/(\mu_0 M_0)$, $\omega_0 = \gamma H_0$ and $\omega_{ac} = \gamma H_{ac}$ in the Eqs. (6) and (7) have a frequency dimension and are, accordingly, related to exchange interaction, magnetic anisotropy and Zeeman interaction with the external dc and ac magnetic fields.

Time evolution of angular coordinates $\vartheta_i = \vartheta_i(t)$ and $\varphi_i = \varphi_i(t)$, that satisfy the system of Eqs. (4) and (5), can be presented as superpositions of the oscillations with frequencies $k\omega$ and amplitudes $(\vartheta_i^k, \varphi_i^k)$ around equilibrium positions $(\vartheta_i^0, \varphi_i^0)$ that are defined by minimums of the function $\bar{U}$. Accordingly, it is convenient to represent a solution of the system of the Eqs. (4) and (5) as Fourier series

$$\vartheta_i(t) = \sum_{k=-\infty}^{\infty} \vartheta_i^k e^{ik\omega t}, \quad \varphi_i(t) = \sum_{k=-\infty}^{\infty} \varphi_i^k e^{ik\omega t}, \quad (8)$$

where we limit ourselves by considering only terms with $k \leq 3$ due to quickly increasing complexity of analytical expressions for the amplitudes $(\vartheta_i^k, \varphi_i^k)$ with an increase of the index k. Since values of the angles $\vartheta_i(t)$ and $\varphi_i(t)$ are real, the Fourier coefficients in Eq. (8) should satisfy the conditions $\vartheta_i^k = (\vartheta_i^{-k})^*$ and $\varphi_i^k = (\varphi_i^{-k})^*$.

By substituting Eq. (8) into the system of Eqs. (4) and (5), taking into account that $|\vartheta_i^0| \gg |\vartheta_i^1| \gg |\vartheta_i^2| \ldots$ and $|\varphi_i^0| \gg |\varphi_i^1| \gg |\varphi_i^2| \ldots$ and grouping summands of the powers of $e^{ik\omega t}$ that have the same smallness, one can obtain a system of equations for the harmonic amplitudes. For $k = 1$, this system is written as

$$(\tau\omega^2 - i\omega\alpha)\vartheta_i^1 + i\omega \sin\vartheta_i^0 \varphi_i^1 - \sum_{j=1,2} (\bar{U}_{\vartheta_i\vartheta_j}\vartheta_j^1 + \bar{U}_{\vartheta_i\varphi_j}\varphi_j^1) = \tilde{U}_{\vartheta_i}, \quad (9)$$

$$-i\omega \sin\vartheta_i^0 \vartheta_i^1 + (\tau\omega^2 - i\omega\alpha)\sin^2\vartheta_i^0 \varphi_i^1 - \sum_{j=1,2} (\bar{U}_{\varphi_i\vartheta_j}\vartheta_j^1 + \bar{U}_{\varphi_i\varphi_j}\varphi_j^1) = \tilde{U}_{\varphi_i}. \quad (10)$$

Here, it is taken into account that $\bar{U}_{\vartheta_i}\big|_{\boldsymbol{\theta}=\boldsymbol{\theta}_0} = 0$ and $\bar{U}_{\varphi_i}\big|_{\boldsymbol{\theta}=\boldsymbol{\theta}_0} = 0$, but $\bar{U}_{\vartheta_i}\big|_{\boldsymbol{\theta}=\boldsymbol{\theta}_0} = 0$ and $\bar{U}_{\varphi_i}\big|_{\boldsymbol{\theta}=\boldsymbol{\theta}_0} = 0$, where $\boldsymbol{\theta}_0 = (\vartheta_1^0, \vartheta_2^0, \varphi_1^0, \varphi_2^0)$ — is a position of the minimum of the function $\bar{U}$ and $\boldsymbol{\theta}(t) = \big(\vartheta_1(t), \vartheta_2(t), \varphi_1(t), \varphi_2(t)\big)$.

It is convenient to represent the equations (9) and (10) in matrix form

$$(\tau\omega^2\mathbf{I} - i\omega\mathbf{D} - \mathbf{U})\boldsymbol{\theta}_1 = \mathbf{F}_1, \quad (11)$$

where $\mathbf{I}$ — is an identity matrix,

$$\mathbf{D} = \begin{pmatrix} \alpha & -\sin\vartheta_1^0 & 0 & 0 \\ \sin^{-1}\vartheta_1^0 & \alpha & 0 & 0 \\ 0 & 0 & \alpha & -\sin\vartheta_2^0 \\ 0 & 0 & \sin^{-1}\vartheta_2^0 & \alpha \end{pmatrix}, \quad (12)$$

$$\mathbf{U} = \begin{pmatrix} \bar{U}_{\vartheta_1\vartheta_1} & \bar{U}_{\vartheta_1\varphi_1} & \bar{U}_{\vartheta_1\vartheta_2} & \bar{U}_{\vartheta_1\varphi_2} \\ \dfrac{\bar{U}_{\varphi_1\vartheta_1}}{\sin^2\vartheta_1^0} & \dfrac{\bar{U}_{\varphi_1\varphi_1}}{\sin^2\vartheta_1^0} & \dfrac{\bar{U}_{\varphi_1\vartheta_2}}{\sin^2\vartheta_1^0} & \dfrac{\bar{U}_{\varphi_1\varphi_2}}{\sin^2\vartheta_1^0} \\ \bar{U}_{\vartheta_2\vartheta_1} & \bar{U}_{\vartheta_2\varphi_1} & \bar{U}_{\vartheta_2\vartheta_2} & \bar{U}_{\vartheta_2\varphi_2} \\ \dfrac{\bar{U}_{\varphi_2\vartheta_1}}{\sin^2\vartheta_2^0} & \dfrac{\bar{U}_{\varphi_2\varphi_1}}{\sin^2\vartheta_2^0} & \dfrac{\bar{U}_{\varphi_2\vartheta_2}}{\sin^2\vartheta_2^0} & \dfrac{\bar{U}_{\varphi_2\varphi_2}}{\sin^2\vartheta_2^0} \end{pmatrix} \quad (13)$$

are system matrices,

$$\mathbf{F}_1 = \begin{pmatrix} \tilde{U}_{\vartheta_1} \\ \sin^{-2}\vartheta_1^0 \tilde{U}_{\varphi_1} \\ \tilde{U}_{\vartheta_2} \\ \sin^{-2}\vartheta_2^0 \tilde{U}_{\varphi_2} \end{pmatrix} \quad (14)$$

is a free vector, and

$$\boldsymbol{\theta}_1 = \begin{pmatrix} \vartheta_1^1 \\ \varphi_1^1 \\ \vartheta_2^1 \\ \varphi_2^1 \end{pmatrix} \quad (15)$$

is a vector of sought amplitudes in Eq. (8)

Similarly, we obtain matrix equations for the vectors $\boldsymbol{\theta}_k$, which are generally written as

$$(\tau k^2\omega^2\mathbf{I} - ik\omega\mathbf{D} - \mathbf{U})\boldsymbol{\theta}_k = \mathbf{F}_k. \quad (16)$$

The expressions for the free vectors $\mathbf{F}_k$ when $k = 2$ and $k = 3$ are provided in the Appendix. Equation (16) is formally solved as

$$\boldsymbol{\theta}_k = (\tau k^2\omega^2\mathbf{I} - ik\omega\mathbf{D} - \mathbf{U})^{-1}\mathbf{F}_k. \quad (17)$$

3. Components of the AFM magnetic susceptibility tensor

The vectors $\boldsymbol{\theta}_k$ in Eq. (17) are used to calculate the components of the susceptibility tensor $\hat{\chi}^{(k)} = \hat{\chi}'^{(k)}(\omega) - i\hat{\chi}''^{(k)}(\omega)$ of the n-th order, which are coefficients in expansion of the Cartesian components of the magnetization vector M_x, M_Y and M_Z along the powers of $e^{ik\omega t}$

$$M_X(t) = M_0 \sum_{i=1,2} \sin\left(\sum_{k=0}^{\infty} \vartheta_i^k e^{ik\omega t}\right) \cos\left(\sum_{k=0}^{\infty} \varphi_i^k e^{ik\omega t}\right)$$

$$= M_X^C + \sum_{k=1}^{\infty} \chi_{XZ}^{(k)}(\omega) H_{ac}^k e^{ik\omega t}, \quad (18)$$

$$M_Y(t) = M_0 \sum_{i=1,2} \sin\left(\sum_{k=0}^{\infty} \vartheta_i^k e^{ik\omega t}\right) \sin\left(\sum_{k=0}^{\infty} \varphi_i^k e^{ik\omega t}\right)$$

$$= M_Y^C + \sum_{k=1}^{\infty} \chi_{YZ}^{(k)}(\omega) H_{ac}^k e^{ik\omega t}, \quad (19)$$

$$M_Z(t) = M_0 \sum_{i=1,2} \cos\left(\sum_{k=0}^{\infty} \vartheta_i^k e^{ik\omega t}\right)$$

$$= M_Z^C + \sum_{k=1}^{\infty} \chi_{ZZ}^{(k)}(\omega) H_{ac}^k e^{ik\omega t}, \quad (20)$$

where M_X^C, M_Y^C and M_Z^C are time-independent parts of the vector $\mathbf{M}$, which are determined as

$$M_X^C = M_0 \sum_{i=1,2} \sin\vartheta_i^0 \cos\varphi_i^0, \quad (21)$$

$$M_Y^C = M_0 \sum_{i=1,2} \sin\vartheta_i^0 \sin\varphi_i^0, \quad (22)$$

$$M_Z^C = M_0 \sum_{i=1,2} \cos\vartheta_i^0. \quad (23)$$

By expressing $\chi_{GZ}^{(1)}(\omega)$ $(G = X, Y, Z)$ through elements of the vector $\boldsymbol{\theta}_1$ by means of Eqs. (18)–(20), we obtain the following Eq. in a linear approximation

$$\chi_{XZ}^{(1)}(\omega) H_{ac} = M_0 \sum_{i=1,2} (\vartheta_i^1 \cos\vartheta_i^0 \cos\varphi_i^0 - \varphi_i^1 \sin\vartheta_i^0 \sin\varphi_i^0), \quad (24)$$

$$\chi_{YZ}^{(1)}(\omega) H_{ac} = M_0 \sum_{i=1,2} (\vartheta_i^1 \cos\vartheta_i^0 \sin\varphi_i^0 + \varphi_i^1 \sin\vartheta_i^0 \cos\varphi_i^0), \quad (25)$$

$$\chi_{ZZ}^{(1)}(\omega) H_{ac} = -M_0 \sum_{i=1,2} \vartheta_i^1 \sin\vartheta_i^0. \quad (26)$$

Here, the dependence on the frequency ω is contained in the elements of the vector $\boldsymbol{\theta}_1$ (see Eq. (17)). Equations (17) and (24)–(26) make it possible to numerically calculate the components of the linear susceptibility tensor. Results of calculation of the real and imaginary parts of $\chi_{ZZ}^{(1)}(\omega)$ are shown in Figure 2 for the following values of the parameters: $\alpha = 0.01$, $\omega_K\tau = 0.005$, $\omega_\Lambda/\omega_K = 10$ and $\omega_0/\omega_K = 0.1, 1.5, 3$. In the weak external field, we observe precession of the total magnetization of the AFM sublattices as a single vector, resulting in the appearance of only one resonance peak both in the antiferromagnetic resonance range and in the NR range (the curve *1* in Figure 2, *b*). With an increase of the external field, both ranges manifest two resonance peaks. Frequencies of the antiferromagnetic resonances can be estimated as $\omega_\pm^p \sim \sqrt{\omega_K(2\omega_\Lambda + \omega_K)} \pm \omega_0$ [27]. Frequencies of the weaker NRs are estimated as $\omega_\pm^n \sim \tau^{-1} + \omega_K + \omega_\Lambda \pm \omega_0$ [27]. Frequency separation between the peaks decreases as the magnitude of the external field H_0 decreases, and they merge when $H_0 = 0$. These results comply with the results of Refs. [26,27]. It should be noted that for $\chi_{YZ}^{(1)}(\omega)$ a zero value is obtained. A similar result is obtained when calculating nonlinear FM susceptibility [38] and leads to an important effect of signal frequency doubling, which will be described by us as an example of the calculation of second-order nonlinear susceptibility.

By expressing the components of the second-order nonlinear susceptibility tensor $\chi_{GZ}^{(2)}(\omega)$ $(G = X, Y, Z)$ through elements of the vectors $\boldsymbol{\theta}_1$ and $\boldsymbol{\theta}_2$ by means of

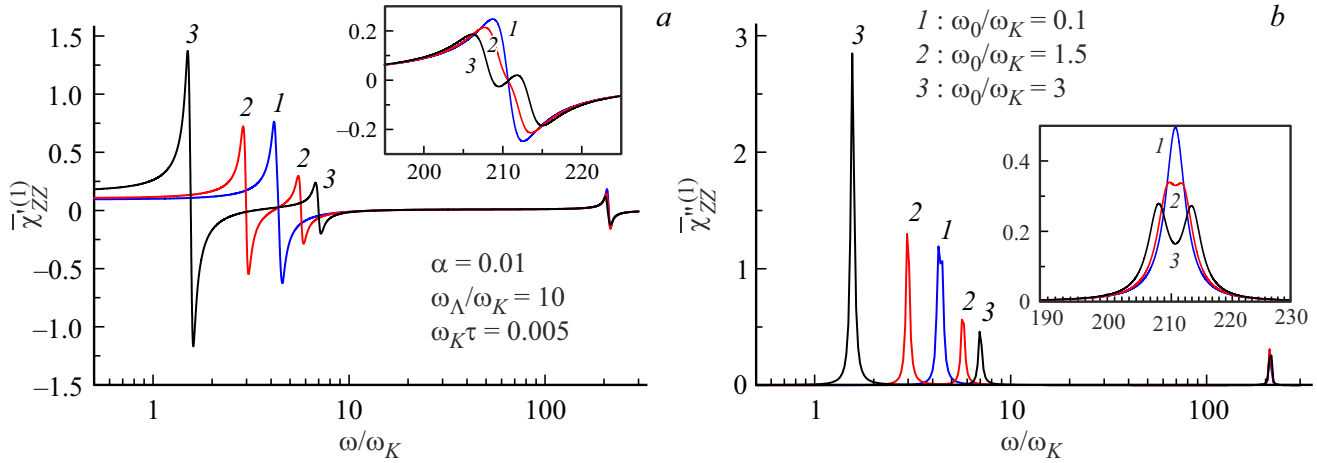

Figure 2. Real $\bar{\chi}'^{(1)}_{ZZ}$ (a) and imaginary $\bar{\chi}''^{(1)}_{ZZ}$ (b) parts of the component of the normalized linear susceptibility tensor $\bar{\chi}^{(1)}_{ZZ} = \chi^{(1)}_{ZZ} H_K/M_0$ (Eq. (24)) vs the frequency ω/ω_K for $\alpha = 0.01$, $\omega_K\tau = 0.005$, $\omega_\Lambda/\omega_K = 10$ and various values of ω_0/ω_K.

Eqs. (18)–(20), we obtain the following

$$\chi^{(2)}_{XZ}(\omega)H^2_{ac} = M_0 \sum_{i=1,2}\left(\vartheta_i^2 \cos\vartheta_i^0 \cos\varphi_i^0 - \varphi_i^2 \sin\vartheta_i^0 \sin\varphi \right.$$
$$\left. - \frac{(\vartheta_i^1)^2 + (\varphi_i^1)^2}{2} \sin\vartheta_i^0 \cos\varphi_i^0 - \vartheta_i^1\varphi_i^1 \cos\vartheta_i^0 \sin\varphi_i^0\right), \quad (27)$$

$$\chi^{(2)}_{YZ}(\omega)H^2_{ac} = M_0 \sum_{i=1,2}\left(\vartheta_i^2 \cos\vartheta_i^0 \sin\varphi_i^0 + \varphi_i^2 \sin\vartheta_i^0 \cos\varphi_i^0 \right.$$
$$\left. - \frac{(\vartheta_i^1)^2 + (\varphi_i^1)^2}{2} \sin\vartheta_i^0 \sin\varphi_i^0 + \vartheta_i^1\varphi_i^1 \cos\vartheta_i^0 \cos\varphi_i^0\right), \quad (28)$$

$$\chi^{(2)}_{ZZ}(\omega)H^2_{ac} = M_0 \sum_{i=1,2}\left(-\frac{(\vartheta_i^1)^2}{2} \cos\vartheta_i^0 - \vartheta_i^2 \sin\vartheta_i^0\right). \quad (29)$$

A solution of Eq. (17) when $k = 1, 2$ and substitution of this solution into Eqs. (27)–(29) facilitates the numerical calculation of the components of the second-order susceptibility tensor. The calculation shows that here it is the opposite to the linear susceptibility case, namely, $\chi^{(2)}_{ZZ}(\omega) = 0$, whereas $\chi^{(2)}_{YZ}(\omega) \neq 0$. Thus, the stationary magnetization response along the easy axis of the AFM sublattices to the ac field of frequency ω is observed at a double frequency 2ω, namely, $M_Y(t) - M^C_X = \chi^{(2)}_{YZ}(\omega)H^2_{ac}e^{i2\omega t} + \ldots$. This phenomenon is well studied for the FMs and the AFMs at the frequencies near the ferromagnetic and antiferromagnetic resonances [7]. It is important to note that here we observe this effect in the AFMs at frequencies near the NR. In this case, we see a direct analogy with the same effect that was previously described by us in the FMs at extremely high frequencies [38]. This analogy is related to the similar geometry of the problem, i.e. in the weak external dc field directed along the easy axis of the sublattices, a location of the minimum of the function of density of magnetic energy (without taking into account the ac field) of the ferromagnetic-type sublattices corresponds to a location of the minimum of this function in the FMs at the same direction of the dc field. With an increase of the value of the dc field, the location of the minimums of the function of density of AFM magnetic energy is changed, which causes various states of the AFMs to depend on the value and the direction of the external dc field [7,27]. Manifestation of the nonlinear effects in other states of the antiferromagnetics requires separate studies.

The components of the third-order nonlinear susceptibility tensor $\chi^{(3)}_{GZ}(\omega)$ $(G = X, Y, Z)$ are obtained from Eqs. (17) and (24)–(26) when $k = 3$, namely,

$$\chi^{(3)}_{XZ}(\omega)H^3_{ac} = M_0 \sum_{i=1,2}\left[-(\vartheta_i^2\varphi_i^1 + \vartheta_i^1\varphi_i^2)\cos\vartheta_i^0 \sin\varphi_i^0 \right.$$
$$- (\vartheta_i^1\vartheta_i^2 + \varphi_i^1\varphi_i^2)\sin\vartheta_i^0 \cos\varphi_i^0$$
$$+ \left(\vartheta_i^3 - \frac{(\vartheta_i^1)^3}{6} - \frac{1}{2}\vartheta_i^1(\varphi_i^1)^2\right)\cos\vartheta_i^0 \cos\varphi_i^0$$
$$\left. - \left(\varphi_i^3 - \frac{(\varphi_i^1)^3}{6} - \frac{1}{2}(\vartheta_i^1)^2\varphi_i^1\right)\sin\vartheta_i^0 \sin\varphi_i^0\right], \quad (30)$$

$$\chi^{(3)}_{YZ}(\omega)H^3_{ac} = M_0 \sum_{i=1,2}\left[-(\vartheta_i^1\vartheta_i^2 + \varphi_i^1\varphi_i^2)\sin\vartheta_i^0 \sin\varphi_i^0 \right.$$
$$+ (\vartheta_i^2\varphi_i^2 + \vartheta_i^1\varphi_i^2)\cos\vartheta_i^0 \cos\varphi_i^0$$
$$+ \left(\vartheta_i^3 - \frac{(\vartheta_i^1)^3}{6} - \frac{1}{2}\vartheta_i^1(\varphi_i^1)^2\right)\cos\vartheta_i^0 \sin\varphi_i^0$$
$$\left. + \left(\varphi_i^3 - \frac{(\varphi_i^1)^3}{6} - \frac{1}{2}(\vartheta_i^1)^2\varphi_i^1\right)\sin\vartheta_i^0 \cos\varphi_i^0\right], \quad (31)$$

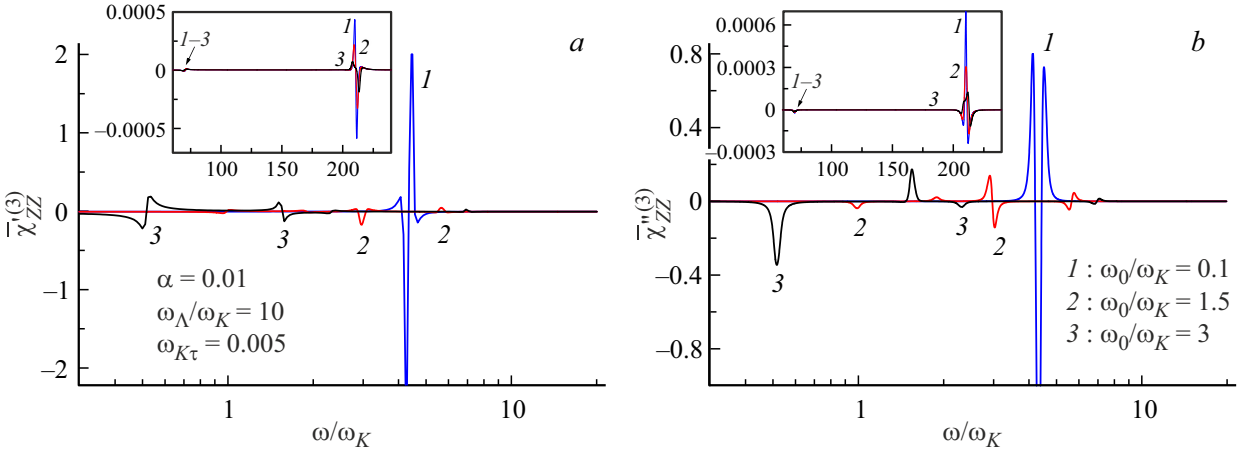

Figure 3. Real $\bar{\chi}'^{(3)}_{ZZ}$ (a) and imaginary $\bar{\chi}''^{(3)}_{ZZ}$ (b) components of the normalized third-order susceptibility tensor $\bar{\chi}^{(3)}_{ZZ} = \chi^{(3)}_{ZZ} H_K^3/M_0$ (Eq. (24)) vs the frequency ω/ω_K for $\alpha = 0.01$, $\omega_K\tau = 0.005$, $\omega_\Lambda/\omega_K = 10$ and various values of ω_0/ω_K.

$$\chi^{(3)}_{ZZ}(\omega)H^3_{ac} = M_0 \sum_{i=1,2}\left(\left(\frac{(\vartheta_i^1)^3}{6} - \vartheta_i^3\right)\sin\vartheta_i^0 - \vartheta_i^1\vartheta_i^2\cos\vartheta_i^0\right). \tag{32}$$

Frequency dependencies of the real and imaginary parts $\chi^{(3)}_{ZZ}(\omega)$ for $\alpha = 0.01$, $\omega_K\tau = 0.005$, $\omega_\Lambda/\omega_K = 10$ and $\omega_0/\omega_K = 0.1, 1.5, 3$ are shown in Figure 3.

Note that $\chi^{(3)}_{XX}(\omega)$ includes an additional NR subharmonic when $\omega = \omega_{NR}/3$ (see inserts in Figure 3). Generation of the subharmonics is similar to manifestation of subharmonics in nonlinear oscillations under the effect of an external oscillating force [55].

4. Dynamic magnetic hysteresis at the ultra-high frequencies

DMH is induced by the external ac field and is of high practical importance, since this field causes heating in the magnetic materials [2–4]. Visually, a DMH loop is a flat parametric curve in rectangular coordinates. It is convenient to display a normalized value of the external ac field $h(t) = \mathrm{Re}[H_{ac}(t)]/H_{ac} = \cos\omega t$ along the abscissa axis of these coordinates and a normalized value of the Cartesian component of magnetization $m(t) = \mathrm{Re}[M_G(t)]/M_0$ along the ordinate axis, where t varies within a period of oscillations $T = 2\pi/\omega$, while an index $G = X, Y, Z$ characterizes the considered component of the magnetization vector **M**. The area of the DMH loop is related to the energy absorbed by the material during the period T, whereas the form, the slope and the location of the geometric center of the loop depend both on the value of the external dc field and the value and the frequency of the external ac field [38,47]. While DMH is well studied both in the low-frequency part of the spectra of the magnetic materials and in the range of the ferromagnetic and antiferromagnetic resonances [38,47,56], it was almost unstudied at the extremely high frequencies. DMH data

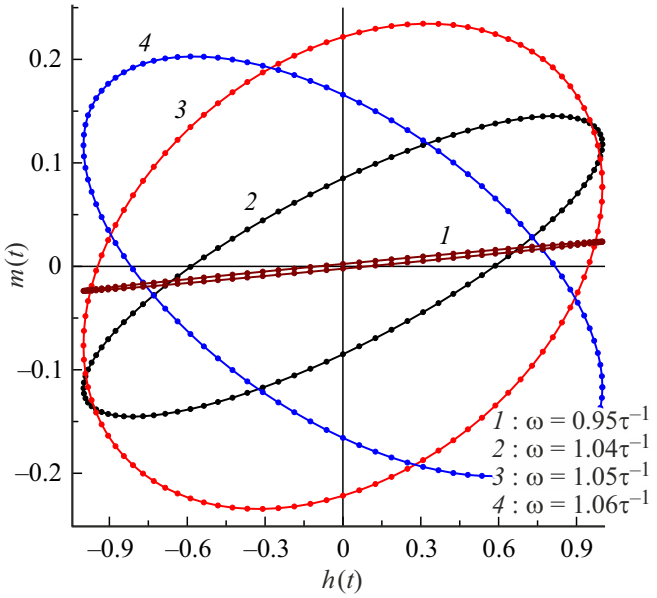

Figure 4. DMH for $\alpha = 0.01$, $\omega_K\tau = 0.005$, $\omega_\Lambda/\omega_K = 10$, $\omega_0/\omega_K = 0.1$, $\omega_{ac}/\omega_K = 0.5$ and various values of the frequency of the ac field ω (the NR range).

for the ferromagnetic nanoparticles at frequencies within the NR range are provided in Ref. [38]. Here, we provide results of DMH calculations at the extremely high frequencies for the antiferromagnetic particles.

Equation (18) allows one to obtain an image of the hysteresis loop when $G = X$, which is shown in Figures 4–7. In Figure 4, the frequency of the ac field ω is varied within the NR range. It is clearly seen that with distance of the field frequency from the NR frequency $\omega_{NR} \sim \tau^{-1}$ the loop collapses, which is caused by a decrease of absorption of electromagnetic energy away from the resonance line and, as a result, by a decrease of the area of the DMH loop.

Away from the resonance line the DMH loop degenerates into a line segment.

The role of the dc field is clearly shown in Figure 5, where the value of the external dc field is a varied parameter. With the increase of the value of the external field, there is an observed shift of the absorption maximum (see Figure 2). As the frequency at which the DMG is observed moves away from the absorption maximum, the loop area decreases. This effect is similar to the effect in Figure 4, the only difference

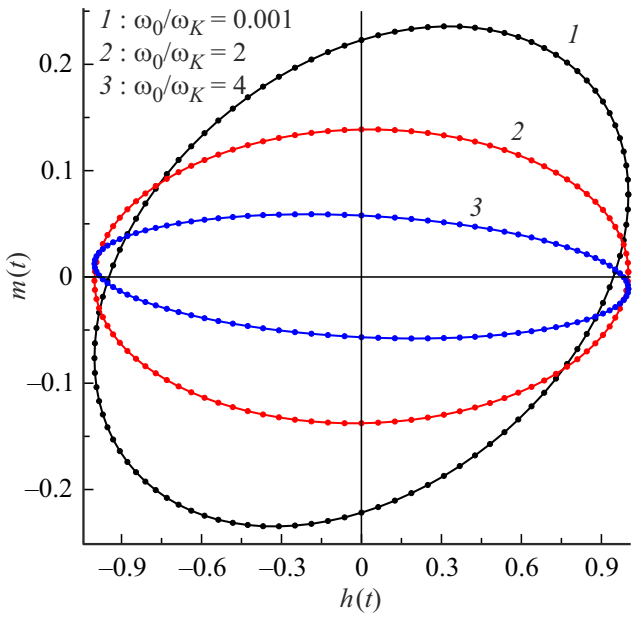

Figure 5. DMH for $\alpha = 0.01$, $\omega_K\tau = 0.005$, $\omega_\Lambda/\omega_K = 10$, $\omega\tau = 1.05$, $\omega_{ac}/\omega_K = 0.5$ and various values of the frequency ω_0.

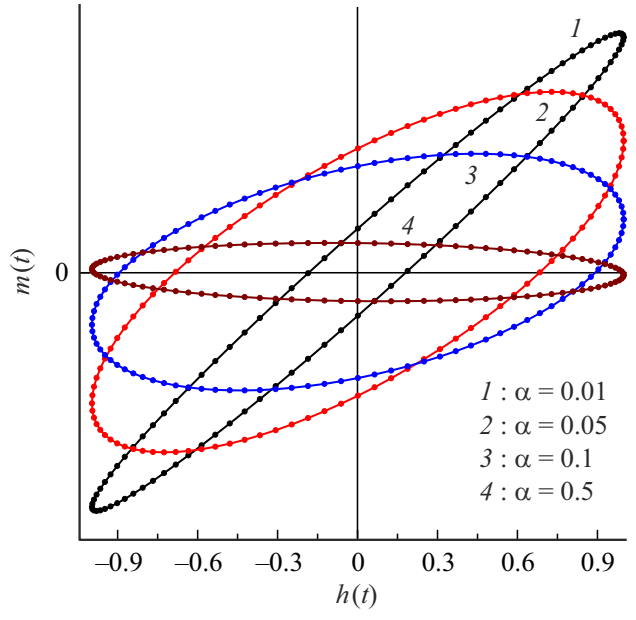

Figure 6. DMH for $\omega\tau = 1$, $\omega_K\tau = 0.05$, $\omega_\Lambda/\omega_K = 10$, $\omega_0/\omega_K = 1$, $\omega_{ac}/\omega_K = 0.5$ and various values of the parameter α.

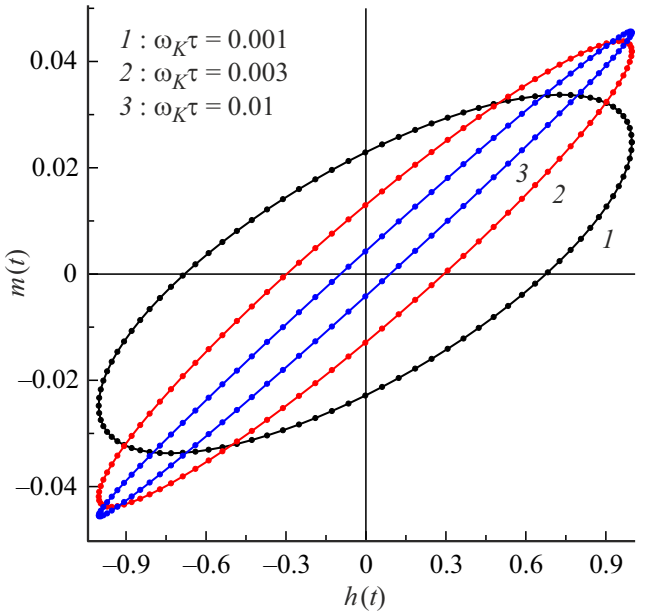

Figure 7. DMH for $\alpha = 0.01$, $\omega\tau = 1$, $\omega_\Lambda/\omega_K = 10$, $\omega_0/\omega_K = 1$, $\omega_{ac}/\omega_K = 0.5$ and various values of the time of inertial relaxation τ.

being that in Figure 4 the distance from a carrier frequency to the resonance frequency is changed by varying the carrier frequency, whereas here the change is accomplished by varying the resonance frequency by means of the external field. Dependences of the NR frequencies in the AFMs on the external field are described in the study [27].

Figure 6 shows the influence of variation of the decay parameter on the DMH form. Since the decay parameter determines a half-width of the absorption line, then its increase results in an increase of absorption at the frequency that is close to the resonance one. As a result, the area of the DMH loop increases. However, with the increase of the line half-width its amplitude decreases. With noticeable reduction of absorption, the loop area decreases again, which is demonstrated in Figure 6. Finally, Figure 7 shows a DMH dependence on the time of inertia relaxation. This parameter determines the NR frequency $\omega_{NR} \sim \tau^{-1}$, therefore, with a decrease of τ ω_{NR}, increases and the distance between the probing and resonance frequencies increases. It is the same effect as in Figure 5, but now it is induced by varying the resonance frequency not by the external field, but by varying the time of inertial relaxation. With increasing distance, absorption drops and the area of the DMH loop is reduced.

In the weak external dc field that are directed along the easy axis of the AFM sublattices, the positions of the minimums of the functions of density of magnetic energy of the AFM sublattices are arranged similar to the minimums of the functions of density of FM magnetic energy. In this case, the area and the slope of the AFM DMH loop can be evaluated by formulas provided in Ref. [38] (see also Ref. [47]) for the FMs.

5. Conclusion

We have investigated the nonlinear stationary response to the ac field of the magnetization of an AFM that is under the combined effect of ac and dc fields. The field of applicability of previous studies of the nonlinear effects in antiferromagnetic nanoparticles is limited by the use of the LLG equation, which does not take into account inertial effects and does not make it possible to reproduce the NR in the magnetic susceptibility spectra at extremely high frequencies. As shown by recent studies [18–32], in order to investigate superfast relaxation processes and the properties of magnetic materials, which are manifested in the magnetic fields of extremely high frequency, where the inertial effect play a significant role, it is necessary to use the generalized inertial LLG equation. Using the method of successive approximations, the inertial LLG equations that describe the dynamics of the magnetizations of the identical AFM sublattices were solved to deduce analytical expressions for the components of the second- and third-order nonlinear susceptibility tensor. At the same time, the expressions obtained for the linear part of susceptibility are in full agreement with independent studies [26,27]. Some nonlinear effects that are well studied in the frequency range of AFM resonance, such as resonances at frequencies which are multiples of the ac field frequency as well as the appearance of an ac component of the magnetization at double the frequency of the external ac field, are reproduced within the AFM NR range. These nonlinear effects are caused by the presence of anisotropy in magnetic media and the nonlinearity of the LLG equation. The inertial term introduced into the LLG equation both phenomenologically [18,22] and derived based on theoretical consideration of this phenomenon microscopically [33–37], results in the presence of eigen (nutation) oscillations at extremely high frequencies. In turn, the presence of a dissipative term in the LLG equation causes the damping of the eigen oscillations of magnetization, while forced oscillations have a finite amplitude when an exciting frequency coincides with the eigen frequency, and a finite width of the resonance lines. The calculations presented are true for the antiferromagnetic particles. The results can be generalized for considering magnetic characteristics of thin antiferromagnetic films and bulk AFMs when the specifics of the problem allow the use of a simplified expression for the magnetic energy (3) (for example, without taking into account spin waves, heterogeneous magnetization of the samples, etc.).

DMH is calculated at the extremely high frequencies that correspond to the NR range (see Figures 4–7). It is shown that nonlinear susceptibility and the DMH form significantly depend on the values of the dc and ac fields as well as on dynamic parameters of the magnetization, for example, the times of inertial relaxation. The results can be used for practical applications, such as modeling and interpretation of superfast switching processes [16,17]. Besides, by estimating the hysteresis area, one can judge heating properties of the magnetic nanoparticles under the effect of extremely high-frequency fields. Finally, detecting the additional resonances that occur in the strong ac fields at extremely high frequencies in the AFM spectra can be the object of future experimental studies.

Appendix

The vector $\mathbf{F}_2$ in Eq. (16) when $k = 2$ is written as

$$\mathbf{F}_2 = \begin{pmatrix} a_1 + R_{\vartheta_1} \\ b_1 + R_{\varphi_1} \\ a_2 + R_{\vartheta_2} \\ b_2 + R_{\varphi_2} \end{pmatrix} + \tilde{\mathbf{U}}\boldsymbol{\theta}_1, \tag{33}$$

where the elements a_i, b_i and R_{x_i} are defined as

$$a_i = -\varphi_i^1 \left(i\omega\vartheta_i^1 \cos\vartheta_i^0 - \frac{1}{2}\tau\omega^2\varphi_i^1 \sin 2\vartheta_i^0 \right), \tag{34}$$

$$b_i = -(2\tau\omega^2 - i\omega\alpha)\vartheta_i^1\varphi_i^1 \sin 2\vartheta_i^0 - i\omega(\vartheta_i^1)^2 \cos\vartheta_i^0, \tag{35}$$

$$R_{x_i} = \frac{1}{2}\sum_{j,k=1,2} \Big(\bar{U}_{x_i\vartheta_j\vartheta_k}\vartheta_j^1\vartheta_k^1 + \bar{U}_{x_i\varphi_j\varphi_k}\varphi_j^1\varphi_k^1 + \bar{U}_{x_i\vartheta_j\varphi_k}\vartheta_j^1\varphi_k^1 + \bar{U}_{x_i\varphi_j\vartheta_k}\varphi_j^1\vartheta_k^1 \Big). \tag{36}$$

The matrix $\tilde{\mathbf{U}}$ in Eq. (33) is derived from the matrix $\mathbf{U}$ (see Eq. (13)) by replacement $\bar{U} \to \tilde{U}$ in the latter.

The vector $\mathbf{F}_3$ in Eq. (16) when $k = 3$ is represented as

$$\mathbf{F}_3 = \begin{pmatrix} c_1 + \tilde{R}_{\varphi_1} + P_{\vartheta_1} \\ d_1 + \tilde{R}_{\varphi_1} + P_{\varphi_1} \\ c_2 + \tilde{R}_{\vartheta_2} + P_{\vartheta_2} \\ d_2 + \tilde{R}_{\varphi_2} + P_{\varphi_2} \end{pmatrix}, \tag{37}$$

where the elements $\tilde{R}_{x_i}$ are derived from the elements R_{x_i} by replacement $\bar{U} \to \tilde{U}$ in the latter, while the elements c_i, d_i and P_{x_i} are defined as

$$c_i = \tau\omega^2\varphi_i^1(\vartheta_i^1\varphi_i^1 \cos 2\vartheta_i^0 + 2\varphi_i^2 \sin 2\vartheta_i^0) - i\omega\left[(\vartheta_i^2\varphi_i^1 + 2\vartheta_i^1\varphi_i^2)\cos\vartheta_i^0 - \frac{1}{2}(\vartheta_i^1)^2\varphi_i^1 \sin\vartheta_i^0 \right], \tag{38}$$

$$d_i = 3i\omega\vartheta_i^1\vartheta_i^2 \cos\vartheta_i^0 - \frac{1}{2}i\omega(\vartheta_i^1)^3 \sin\vartheta_i^0 - (3\tau\omega^2 - i\omega\alpha) \times \left[(\vartheta_i^1)^2\varphi_i^1 \cos 2\vartheta_i^0 + (\vartheta_i^2\varphi_i^1 + 2\vartheta_i^1\varphi_i^2)\sin 2\vartheta_i^0 \right], \tag{39}$$

$$P_{x_i} = \sum_{j,k=1,2} \big(\bar{U}_{x_i\vartheta_j\vartheta_k}\vartheta_j^1\vartheta_k^2 + \bar{U}_{x_i\varphi_j\varphi_k}\varphi_j^1\varphi_k^2 + \bar{U}_{x_i\vartheta_j\varphi_k}\vartheta_j^1\varphi_k^2 + \bar{U}_{x_i\varphi_j\vartheta_k}\varphi_j^1\vartheta_k^2 \big) + \frac{1}{6}\sum_{j,k,l=1,2} \big(\bar{U}_{x_i\vartheta_j\varphi_k\varphi_l}\vartheta_j^1\varphi_k^1\varphi_l^1 + \bar{U}_{x_i\varphi_j\vartheta_k\varphi_l} \times \varphi_j^1\vartheta_k^1\varphi_l^1 + \bar{U}_{x_i\varphi_j\varphi_k\vartheta_l}\varphi_j^1\varphi_k^1\vartheta_l^1 + \bar{U}_{x_i\varphi_j\varphi_k\varphi_l}\varphi_j^1\varphi_k^1\varphi_l^1 + \bar{U}_{x_i\varphi_j\vartheta_k\vartheta_l}\varphi_j^1\vartheta_k^2\vartheta_l^1 + \bar{U}_{x_i\vartheta_j\varphi_k\vartheta_l}\vartheta_j^1\varphi_k^1\vartheta_l^1 + \bar{U}_{x_i\vartheta_j\vartheta_k\varphi_l}\vartheta_j^1\vartheta_k^1\varphi_l^1 + \bar{U}_{x_i\vartheta_j\vartheta_k\vartheta_l}\vartheta_j^1\vartheta_k^1\vartheta_l^1 \big). \tag{40}$$

Funding

The work was supported by the Russian Science Foundation grant No. 25-22-00119. https://rscf.ru/project/25-22-00119/

Conflict of interest

The authors declare that they have no conflict of interest.

References

[1] A.B. Shick, S. Khmelevskyi, O.N. Mryasov, J. Wunderlich, T. Jungwirth. Phys. Rev. B **81**, 212409 (2010).
[2] A.H. MacDonald, M. Tsoi. Phil. Trans. Royal Soc. A **369**, 3098 (2011).
[3] E.V. Gomonay, V.M. Loktev. Low Temp. Phys. **40**, 17 (2014).
[4] T. Jungwirth, X. Marti, P. Wadley, J. Wunderlich. Nat. Nanotech. **11**, 231 (2016).
[5] O. Gomonay, T. Jungwirth, J. Sinova. Phys. Stat. Sol. RRL. **11**, 1700022 (2017).
[6] V. Baltz, A. Manchon, M. Tsoi, T. Moriyama, T. Ono, Y. Tserkovnyak. Rev. Mod. Phys. **90**, 015005 (2018).
[7] A.G. Gurevich, G.A. Melkov, Magnetization Oscillations and Waves (CRC Press, London, 1996).
[8] A.P. Guimaraães. Principles of Nanomagnetism. Springer, Berlin Heidelberg (2009).
[9] Y.L. Raikher, V.I. Stepanov. ZhETF **134**, 514 (2008). (in Russian).
[10] Q.A. Pankhurst, N.T.K. Thanh, S.K. Jones, J. Dobson. J. Phys. D: Appl. Phys. **42**, 224001 (2009).
[11] P. Němec, M. Fiebig, T. Kampfrath, A.V. Kimel. Nat. Phys. **14**, 229 (2018).
[12] P. Wadley, B. Howells, J. Zelezny, C. Andrews, V. Hills, R.P. Campion, V. Novak, F. Freimuth, Y. Mokrousov, A.W. Rushforth, K.W. Edmonds, B.L. Gallagher, T. Jungwirth. Science **351**, 587 (2016).
[13] A. Kirilyuk, A.V. Kimel, Th. Rasing. Rev. Mod. Phys. **82**, 2731 (2010).
[14] T. Kampfrath, A. Sell, G. Klatt, A. Pashkin, S.F. Mährlein, T. Dekorsy, M. Wolf, M. Fiebig, A. Leitenstorfer, R. Huberet. Nat. Photon. **5**, 31 (2011).
[15] A. Pashkin, A. Sell, T. Kampfrath, R. Huber. New J. Phys. **15**, 065003 (2013).
[16] A. Kimel, B. Ivanov, R. Pisarev, P.A. Usachev, A. Kirilyuk, Th. Rasing. Nature Phys. **5**, 727 (2009).
[17] S. Wienholdt, D. Hinzke, U. Nowak. Phys. Rev. Lett. **108**, 247207 (2012).
[18] M.-C. Ciornei, J.M. Rubí, J.-E. Wegrowe. Phys. Rev. B **83**, 020410(R) (2011).
[19] J.-E. Wegrowe, M.-C. Ciornei. Amer. J. Phys. **80**, 607 (2012).
[20] D. Böttcher, J. Henk. Phys. Rev. B **86**, 020404(R) (2012).
[21] S. Giordano, P.-M. Déjardin. Phys. Rev. B **102**, 214406 (2020).
[22] E. Olive, Y. Lansac, J.-E. Wegrowe. Appl. Phys. Lett. **100**, 192407 (2012).
[23] S.V. Titov, W.J. Dowling, Yu.P. Kalmykov. J. Appl. Phys. **131**, 193901 (2022).
[24] M. Cherkasskii, M. Farle, A. Semisalova. Phys. Rev. B **102**, 184432 (2020).
[25] R. Mondal, L. Rózsa, M. Farle, P.M. Oppeneer, U. Nowak, M. Cherkasskii. J. Magn. Magn. Mater. **579**, 170830 (2023).
[26] R. Mondal, S. Großenbach, L. Rózsa, U. Nowak. Phys. Rev. B **103**, 104404 (2021).
[27] S.V. Titov, A.S. Fedorov, A.S. Titov, N.V. Chukashev, Nutation resonance in different states of an antiferromagnet switched by an external magnetic field, Physics of the Solid State, **67** (1), 143, (2025). doi: 10.61011/PSS.2025.01.60593.283
[28] A.M. Lomonosov, V.V. Temnov, J.-E. Wegrowe. Phys. Rev. B, **104**, 054425 (2021).
[29] S.V. Titov, W.J. Dowling, Y.P. Kalmykov, M. Cherkasskii. Phys. Rev. B, **105**, 214414 (2022).
[30] R. Mondal, L. Rózsa. Phys. Rev. B **106**, 134422 (2022).
[31] K. Neeraj, N. Awari, S. Kovalev, D. Polley, N.Z. Hagström, S. Arekapudi, A. Semisalova, K. Lenz, B. Green, J.-C. Deinert, I. Ilyakov, M. Chen, M. Bawatna, V. Scalera, M. d'Aquino, C. Serpico, O. Hellwig, J.-E. Wegrowe, M. Gensch, S. Bonetti. Nat. Phys. **17**, 245 (2021).
[32] V. Unikandanunni, R. Medapalli, M. Asa, E. Albisetti, D. Petti, R. Bertacco, E.E. Fullerton, S. Bonetti. Phys. Rev. Lett. **129**, 237201 (2022).
[33] D. Thonig, O. Eriksson, M. Pereiro. Sci. Rep. **7**, 931 (2017).
[34] M. Fähnle, D. Steiauf, C. Illg. Phys. Rev. B **84**, 172403 (2011).
[35] S. Bhattacharjee, L. Nordström, J. Fransson. Phys. Rev. Lett. **108**, 057204 (2012).
[36] R. Mondal, M. Berritta, A.K. Nandy, P.M. Oppeneer. Phys. Rev. B **96**, 024425 (2017).
[37] R. Mondal, M. Berritta, P.M. Oppeneer. J. Phys.: Condens. Matter **30**, 265801 (2018).
[38] S.V. Titov, W.J. Dowling, A.S. Titov, A.S. Fedorov. AIP Advances, **14**, 035216 (2024).
[39] Y.L. Raikher, V.I. Stepanov. Adv. Chem. Phys. **129**, 419 (2004).
[40] T. Bitoh, K. Ohba, M. Takamatsu, T. Shirane, S. Chikazawa. J. Magn. Magn. Mater. **154**, 59 (1996).
[41] P. Jönsson, T. Jonsson, J.L. García-Palacios, P. Svedlindh. J. Magn. Magn. Mater. **222**, 219 (2000).
[42] Y.L. Raikher, V.I. Stepanov, R. Perzynski. Physica B: Condensed Matter. **343**, 262 (2004).
[43] Y.L. Raikher, V.I. Stepanov. J. Magn. Magn. Mater. **300**, e311 (2006).
[44] P.M. Déjardin, Y.P. Kalmykov, B.E. Kashevsky, H.El. Mrabti, I.S. Poperechny, Y.L. Raikher, S.V. Titov. J. Appl. Phys. **107**, 073914 (2010).
[45] B. Ouari, S.V. Titov, H. El Mrabti, Yu.P. Kalmykov. J. Appl. Phys. **113**, 053903 (2013).
[46] Yu.P. Kalmykov, S.V. Titov, W.T. Coffey, M. Zarifakis, W.J. Dowling. Phys. Rev. B **99**, 184414 (2019).
[47] W.T. Coffey, Y.P. Kalmykov. The Langevin Equation. 4th edition. World Scientific. Singapore (2017).
[48] I. Klik, Y.D. Yao. J. Appl. Phys. **89**, 7457 (2001).
[49] H. El Mrabti, P.M. Déjardin, S.V. Titov, Yu.P. Kalmykov. Phys. Rev. B **85**, 094425 (2012).
[50] G.T. Landi. J. Appl. Phys. **111**, 043901 (2012).
[51] G.T. Landi. J. Magn. Magn. Mater. **324**, 466, (2012).
[52] N.A. Usov, Yu.B. Grebenshchikov. J. Appl. Phys. **106**, 023917 (2009).
[53] N.A. Usov. J. Appl. Phys. **107**, 123909 (2010).
[54] G. Bertotti, I.D. Mayergoyz, C. Serpico, M. d'Aquino, R. Bonin. J. Appl. Phys. **105**, 07B712 (2009).
[55] L.D. Landau, E.M. Lifshitz, Mechanics, 3rd ed. (Pergamon Press, and Waves 1976).
[56] Yu.P. Kalmykov, B. Ouari, S.V. Titov. J. Appl. Phys. **120**, 053901 (2016).

Translated by M.Shevelev